Smart Structures and Systems, *Vol. 23, No. 4 (2019) 337-345*
DOI: https://doi.org/10.12989/sss.2019.23.4.337

Dynamic behavior of a seven century historical monument reinforced by shape memory alloy wires

Karim Hamdaoui*, Zahira Benadla[a], Houssameddine Chitaoui[b] and Mohammed Elamine Benallal[c]

Department of Civil Engineering, Faculty of technology, University of Tlemcen, B.P. 230, 13000, Chetouane, Tlemcen, Algeria

(Received May 14, 2018, Revised January 19, 2019, Accepted January 26, 2019)

Abstract. This work resumes a research that proposes the use of the technique based on the dissipation energy of the shape memory alloy (SMA) ties. It focuses principally on the assessment of the effectiveness of the use of these smart materials on displacements, accelerations and the stresses of the minaret of the great mosque of Ajloun in Jordan. The 3-D finite element model of the minaret is performed by the ANSYS software. First of all, the proposed model is calibrated and validated according to the experimental results gathered from ambient vibration testing results. Then, a nonlinear transient analysis is considered, when the El-Centro earthquake is used as the input signal. Different simulating cases concerning the location, number and type of SMA devices are proposed in order to see their influence on the seismic response of the minaret. Hence, the results confirm the effectiveness of the proposed SMA device.

Keywords: historical structures; shape memory alloys; energy dissipation; earthquake excitation; dynamic analysis

1. Introduction

The challenge that researchers are overcoming is to maintain buildings standing after an earthquake strike. Last technological innovations based on damping materials have been extensively developed to satisfy the needs of engineering by trying to reduce seismic risk. Among them, dissipaters as SMA are proposed (Heresi *et al.* 2014).

Shape memory alloys have remarkable mechanical properties that can be advantageous for civil engineering applications (Azariani *et al*. 2018, Qiu *et al*. 2018) as for rehabilitation and seismic protection (Contreras *et al.* 2014, Torra *et al.* 2014, Ozbulut and Silwal 2016, Preciado *et al*. 2018). The rehabilitation of world heritage structures remains critical, since lots of them are partially destroyed after the series of earthquakes that have affected them. Several applications have been drawn in order to identify the efficiency of this smart material. In the literature, several innovative techniques based on the use of SMA are available. Recently, a numerical study on the dynamic behavior of an old minaret located in Tlemcen (Algeria) when it was retrofitted by SMA wires was published by the first and the second authors (Hamdaoui and Benadla 2014). The dynamic study of the monument was made under different national seismic excitations in order to confirm the effectiveness of the proposed SMA device.

Another example is the application of pre-stressed SMA devices on an aqueduct in Cyprus (Chrysostomou *et al*. 2008). The devices were applied in order to investigate their effectiveness in providing protection to the monument against probable earthquake excitation effects.

An experimental study on a reduced masonry model reproducing historical buildings was proposed by (Casciati and Hamdaoui 2008). The proposed model has been tested on a shaking table when different number and positions of the pre-tensioned SMA wires were anchored to the model.

The scale tests realized by AlSaleh (AlSaleh *et al*. 2011) on a reduced minaret model with the aim to see the effect of SMA wires on the structure's behavior gave evidence that the proposed process works correctly on minarets.

It is worth noting that SMA helical structures are widely used as interventional medical devices and active actuators (Zhou and You 2015, Mehrabi and Karamooz-Ravari 2015). In a recent study, noval artificial muscle based on shape memory alloy is proposed to mimic the behavior of a natural muscle (Ben Jaber *et al.* 2015).

2. Description of the minaret

2.1 History

The great mosque of Ajloun (Figs. 1 and 2) is one of the oldest mosques in Jordan. It was built in 1247 by the Sultan "Najm Aldine Ayoubi". The original part of this mosque minaret, was built by the Sultan "Addaheir Beber", 16 years after the construction of the mosque (1263). The minaret had a top "cap" at the top of its original part, but it was demolished to introduce the new orthogonal extension, which was built 70 years ago only (Ghawamna 1986).

*Corresponding author, Associate Professor
E-mail: karim@unipv.it
[a] Ph.D.
[b] Ph.D. Student
[c] Civil Engineer

http://www.techno-press.com/journals/sss&subpage=7
ISSN: 1738-1584 (Print), 1738-1991 (Online)

Fig. 1 The great mosque of Ajloun

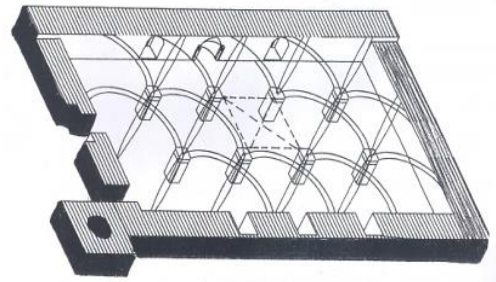

Fig. 2 Horizontal view of the mosque of Ajloun

2.2 Geometric characteristics

The minaret (Figs. 3 and 4) is composed of two parts; the original one made by large and heavy superimposed red stones (without mortar), and the new extension made with the same type as actual Jordan mosques.

The minaret has, in its western side, a small rectangular access door of 1.35*0.72 m^2. It is also equipped with three windows on each side; the lower and the middle one are broad from the outside and narrow from the inside, where the upper one is large and vaulted (Bani-Hani *et al.* 2008).

Inside, a cylindrical column with constant diameter (1.60 m) expands from the level +6.00 m to the end of the original part (+21.00 m). This column continues to extend up to the level of the upper balcony, but with reducing its diameter to 1.40 m (from level +21.00 m to 32.45 m), then to 1.30 m (from level 32.45 to 39.40).

A helical stone stair begins from the level +6.00 m. It is interlocked with the inner minaret stone column and fixed, on its other side, on a common stone column of 25 cm diameter in the center of the minaret. A new similar staircase was made to climb into the added extension. Stairs end in the balcony.

As previously mentioned, the minaret had a "cap" in the end of its original part, but it was destructed to introduce the new octagonal extension. This latter has an intermediate balcony and finished with a new conical helmet.

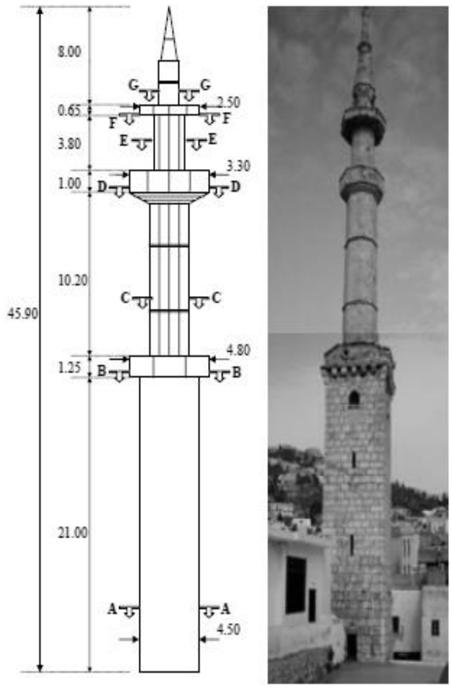

Fig. 3 Vertical of the minaret of Ajloun

Table 1 Mechanical stones properties

Properties	Old materials	New materials
Modulus of elasticity (MPa)	21000	17000
Volume weight (KN/m^3)	26.6	22.3
Resistance to compression (MPa)	19	17
Poisson's coefficient	0.2	0.2

2.3 Mechanical characteristics

The minaret body was made of two types of blocks (original part and new extension). The mechanical properties of the minaret's construction materials were determined in the structural laboratory of the Jordan University of Science and Technology (Hamdaoui 2006).

The used samples were submitted to compression tests to determine their compressive strength and the secant modulus of elasticity. The results are summarized in Table 1.

2.4 Dynamic characteristics

To capture the minaret's dynamic signature, ambient vibration tests were conducted by recording accelerations through sensitive accelerometers. Here; 3 accelerometers were placed at strategic locations, based on a preliminary built finite element model (Bani-Hani *et al.* 2008).

Because of the symmetry of the minaret, directionally uniform excitations are assumed. Output-only model identification technique was then applied to extract the modal signature. The experimentally identified frequencies are given in Table 2.

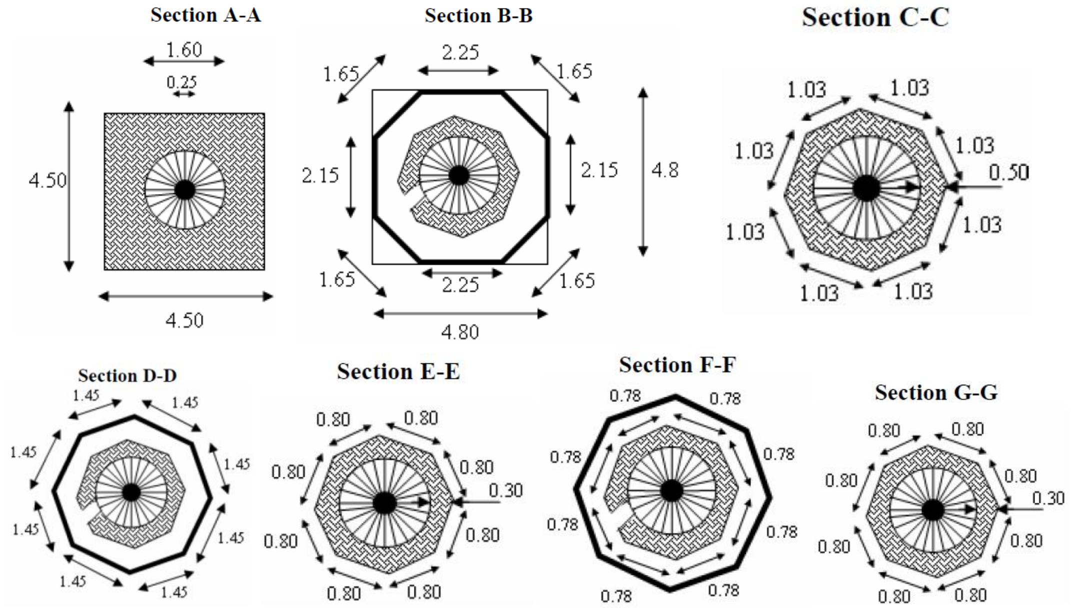

Fig. 4 Different cross-sections of the minaret

Table 2 Experimentally measured frequencies

Accelerometer	1st and 2nd modes	3rd and 4th modes	5th and 6th modes	7th mode	8th and 9th modes
1	1.283	3.369	6.585	9.289	10.968
2	1.285	3.354	6.558	Not detected	10.783
3	1.287	3.356	6.538	9.414	10.861

3. Finite element model

A three-dimensional finite element model is built using the ANSYS software (version 11.0) (ANSYS 2003). The model is built according to the experimentally determined mechanical and dynamic characteristics of the minaret.

In the aim to be as close as possible to a realistic model, an equivalent modulus of elasticity for the whole structure was taking into account. The "E_{eq}" that was calculated based on the construction type of the minaret (superimposed cut stones without any mortar between the stone layers) were around 4300 MPa.

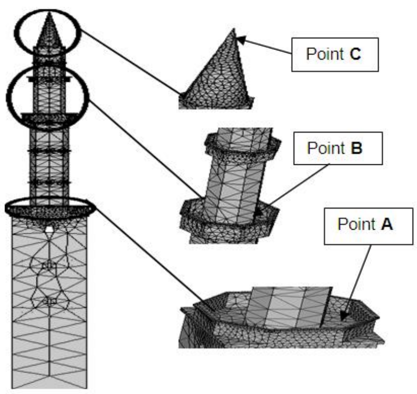

Fig. 5 Minaret in 3-D model

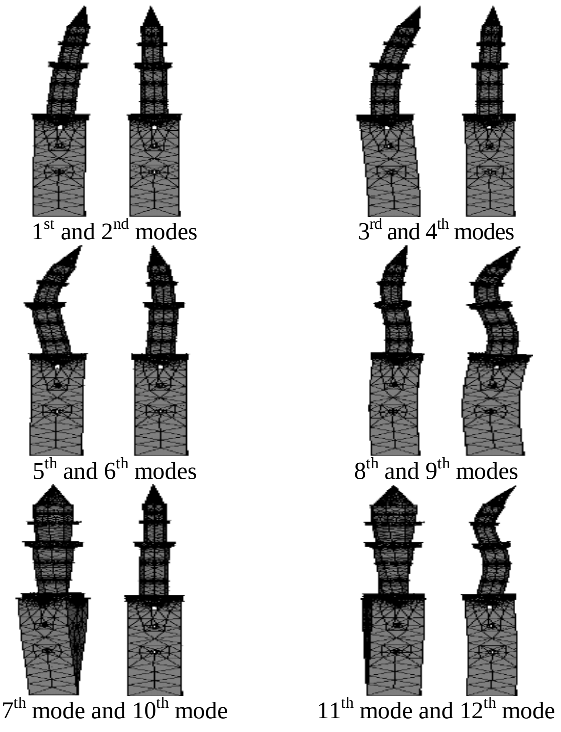

Fig. 6 The first twelve mode shapes

Table 3 Periods and frequencies of the first twelve modes

Modes	Frequencies (Hz)	Period (s)	Direction of mode	Modes	Frequencies (Hz)	Period (s)	Direction of mode
1st	1.286	0.777	x	7th	14.033	0.071	torsion
2nd	1.290	0.775	y	8th	15.365	0.065	y
3rd	3.212	0.311	x	9th	15.398	0.064	x
4th	3.222	0.310	y	10th	16.533	0.06	z
5th	7.181	0.139	x	11th	18.309	0.054	torsion
6th	7.201	0.138	y	12th	20.451	0.048	x

Table 4 Comparison between digital and experimental results

Modes	Frequency (HZ)		Error (%)
	Measured	M.E.F	
1st and 2nd mode	1.285	1.286	0.078
3rd and 4th mode	3.360	3.212	-4.41
5rd and6th mode	6.560	7.181	9.47
7th modes	9.352	14.033	50.05
8rd and 9th mode	10.871	15.366	41.35

A comparison between the experimental results and those numerically obtained is presented in Table 4. From this comparison, one may conclude that the model is relatively representative because the error rate is minor, especially for the first four modes; where the contribution of the modes is usually major for slender cylindrical structures.

4. Characteristics of the materials used for building

SMA as superelastic wires are proposed here for the reinforcement of the minaret. The wires are fixed on their two sides on polygonal steel stiff belts (as the form of the minaret) (Fig. 7), at locations where the stresses are relatively important.

In order to reinforce the minaret, Cu-based SMA wires of 3.5 mm diameter and 1.2 m length are used. Their mechanical characteristics are listed in Table 5. The SMA behavior is characterized by six parameters that define the stress-strain behavior (Fig. 8). These parameters are adopted for room temperature; they are grouped in Table 6.

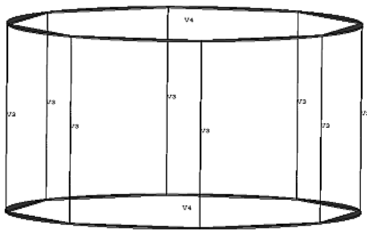

Fig. 7 Assembly of the SMA by the polygonal belts

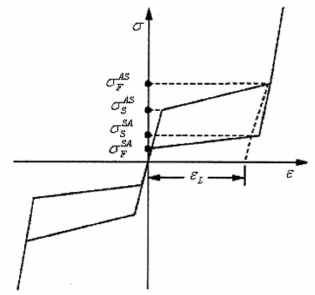

Fig. 8 Superelastic behavior typical of the SMA

Table 5 Characteristic of the SMA properties

σ_S^{AS} (MPa)	σ_F^{AS} (MPa)	σ_S^{SA} (MPa)	σ_F^{SA} (MPa)	ε_L	α
140	270	200	70	0.03	0.27

*SIG-SAS σ_S^{AS}: initial loading stress value
*SIG-FAS σ_F^{AS}: final loading stress value
*SIG-SSA σ_S^{SA}: initial unloading stress value
*SIG-FSA σ_F^{SA}: final unloading stress value
*EPSILON ε_L: maximum residual deformation.
*ALPHA α: compatibility setting of physical responses in tension and compression

Table 6 Mechanical characteristics of the SMA

Modulus of elasticity (MPa)	60000
Coefficient of Poisson	0.3

Table 7 Mechanical characteristics of the polygonal belts

Modulus of elasticity (MPa)	210000
Coefficient of Poisson	0.3

The polygonal stiff belts mechanical characteristics are shown in Table 7.

5. Dynamic analysis of the minaret

A temporal analysis by applying the El-Centro earthquake is carried out in order to study the minaret's behavior first, in its virgin state then after being reinforced with SMA wires. Here, the seismic action is applied in the x direction.

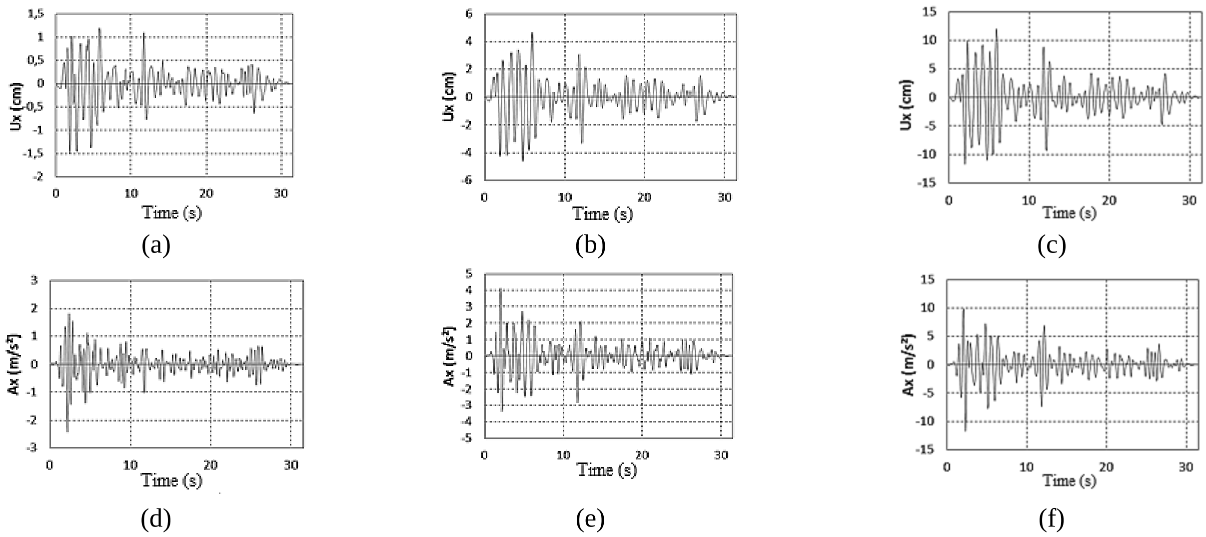

Fig. 10 (a), (b), (c) displacement, (d), (e), (f) acceleration in points A, B, C

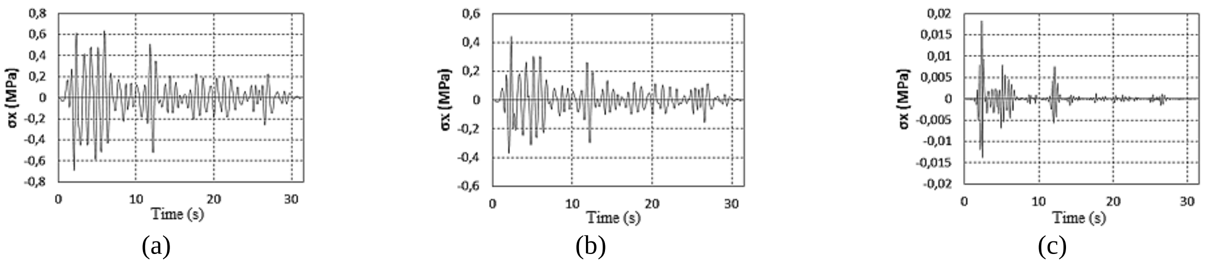

Fig. 11 (a), (b), (c) variation of stress in points A, B, C

The results of calculation without and with SMA led by software ANSYS 11.0 version will be presented, such as displacement, acceleration and distribution of stress.

5.1 Before reinforcement of the minaret

Three reference points (A, B, C) are selected to calculate displacements, accelerations (Fig. 10) and stresses distribution (Fig. 11). These points are selected as the places where the stresses are important. They are located at 21.21 (A), 32.72 (B) and 45.9 (C) meters on the minaret (Fig. 5).

Note that the maximum displacement is found at point C, where the maximum stresses are located at points A and B.

5.2 After reinforcement of the minaret

In the present sub-section, the dynamic analysis is carried out when the minaret is reinforced with four, then eight SMA wire devices positioned in two different locations:

The first, noted "LI": located at a height of 40.46 m. This position is selected since the displacement is maximal at the top of the minaret. The second, noted "LII": located at a height of 22.55 m. This position is selected since an important stress concentration is seen at this level.

Transient analyses are then conducted, at each location and for the two reinforcement cases. The same quantities (displacements, accelerations and stresses) are measured in the same points A, B and C.

Table 8 Comparison between the two proposed devices for the LI location

Number of SMA		4 SMA	8 SMA	Difference
Point	Sizes			(%)
A	Ux_{max} (cm)	1.47536	1.47554	-0.01
	Ax_{max} (m/s²)	2.40015	2.39887	0.05
	σx_{max} (MPa)	0.701905	0.702758	-0.12
B	Ux_{max} (cm)	4.66116	4.66501	-0.08
	Ax_{max} (m/s²)	4.12132	4.12389	-0.06
	σx_{max} (MPa)	0.427192	0.443128	-3.73
C	Ux_{max} (cm)	11.9822	11.9767	0.04
	Ax_{max} (m/s²)	11.5844	11.5835	0.007
	σx_{max} (MPa)	0.018401	0.018288	0.61

Table 8 provides a comparison in term of displacement (Ux), acceleration (Ax) and stress (σx) at the selected points (A, B and C) between the two proposed reinforcement devices (4 then 8 SMA wires) placed in the LI location. According to the results, no big difference is seen in terms of displacement, acceleration and stress for the two proposed cases. One can conclude that the device with 4 SMA has only been sufficient. This will reduce costs and computation time.

The results shown in Table 9, providing the same comparison as the previous table but when the devices are placed in the LII location, confirm that the device with 4 SMA has only been sufficient.

1st location (LI, 40.46 m)

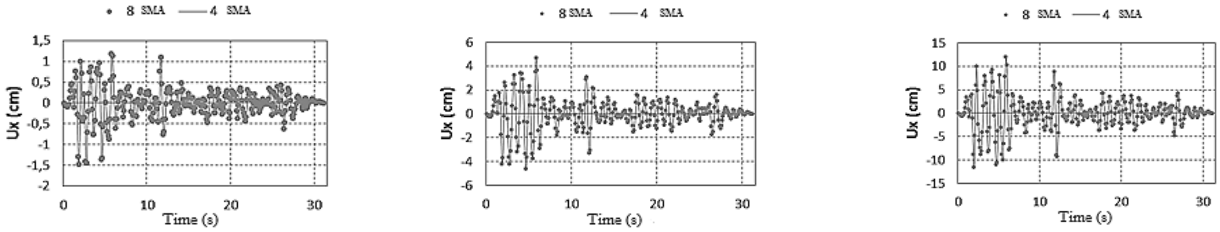

(a) (b) (c)

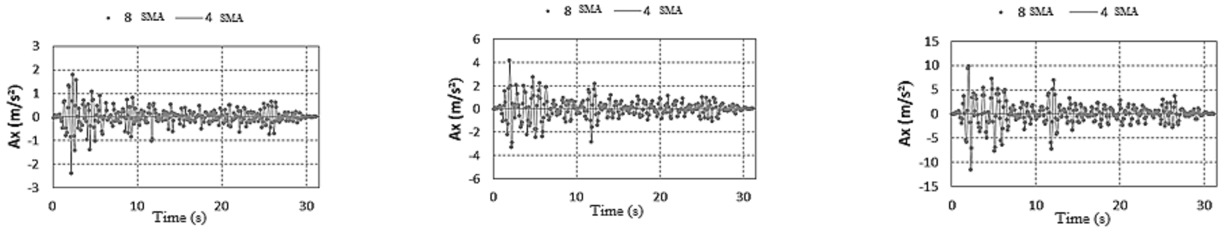

(d) (e) (f)

Fig. 13 (a), (b), (c) displacement, (d), (e), (f) accelerations at points A, B, C

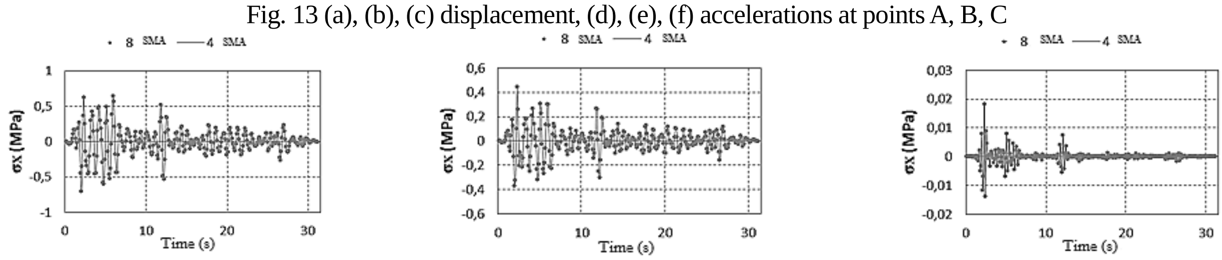

(a) (b) (c)

Fig. 14 (a), (b), (c) variation of stress in points A, B, C

2nd location (LII, 22.55 m)

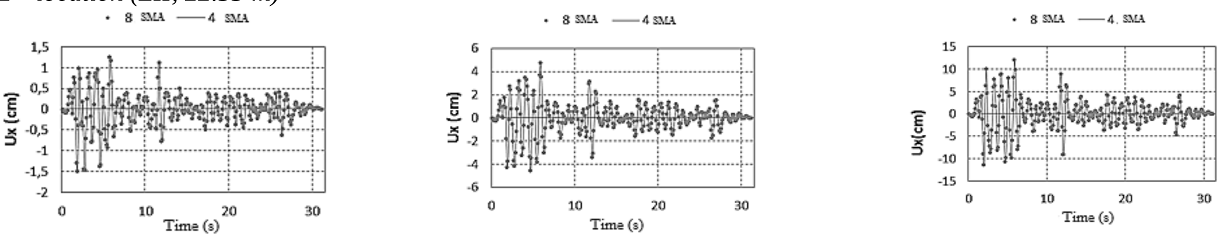

(a) (b) (c)

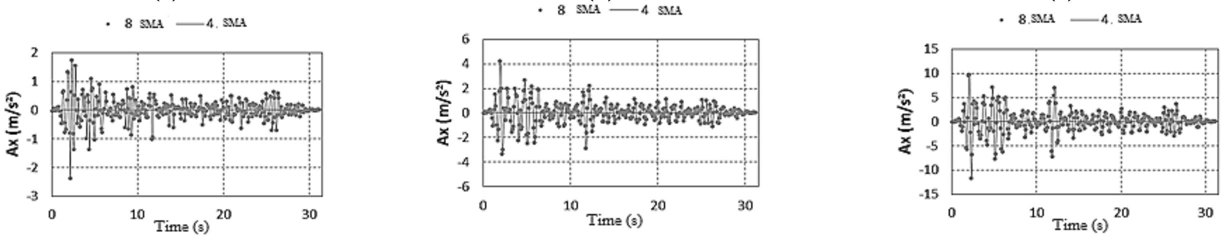

(d) (e) (f)

Fig. 15 (a), (b), (c) displacement, (d), (e), (f) accelerations at points A, B, C

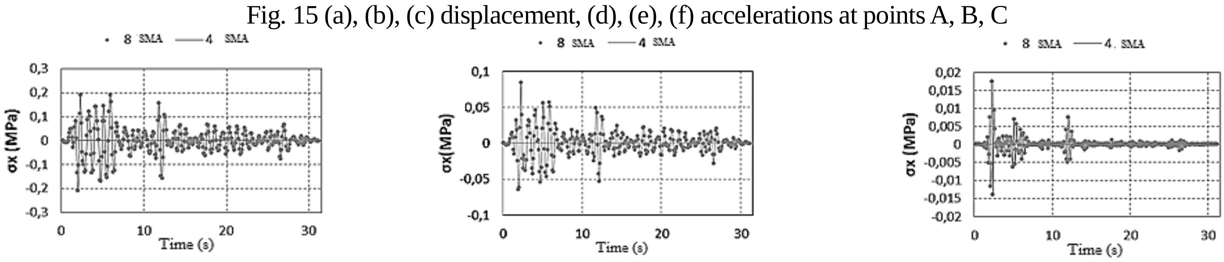

(a) (b) (c)

Fig. 16 (a), (b), (c) variation of stress in points A, B, C

Table 9 Comparison between the two proposed devices for the LII location

Number of SMA		4 SMA	8 SMA	Difference (%)
Point	Sizes			
A	Ux_{max} (cm)	1.49621	1.50014	-0.26
	Ax_{max} (m/s²)	2.38898	2.38778	0.05
	σx_{max} (MPa)	0.213005	0.208043	2.33
B	Ux_{max} (cm)	4.71774	4.71353	0.08
	Ax_{max} (m/s²)	4.18589	4.20078	-0.35
	σx_{max} (MPa)	0.085637	0.084545	1.27
C	Ux_{max} (cm)	11.9321	11.9111	0.17
	Ax_{max} (m/s²)	11.714	11.7803	-0.57
	σx_{max} (MPa)	0.017617	0.017443	0.98

Table 10 Comparison between the two proposed locations (LI and LII)

Location of SMA		1^{st}	2^{nd}	Difference
Point	Sizes	(40.46m)	(22.55m)	(%)
A	Ux_{max} (cm)	1.47536	1.49621	1.4
	Ax_{max} (m/s²)	2.40015	2.38898	-0.47
	σx_{max} (MPa)	0.701905	0.213005	-230
B	Ux_{max} (cm)	4.66116	4.71774	1.2
	Ax_{max} (m/s²)	4.12132	4.18589	1.5
	σx_{max} (MPa)	0.427192	0.085637	-399
C	Ux_{max} (cm)	11.9822	11.9321	-0.42
	Ax_{max} (m/s²)	11.5844	11.714	1.11
	σx_{max} (MPa)	0.018401	0.017617	-4.45

In Table 10, a comparison is drawn between the two proposed positions of the 4 SMA reinforcing device (LI and LII locations). First of all, it is seen that the difference in term of displacements and accelerations is negligible (the maximum difference is around 1.5% only). For the stresses, the difference is clearly visible; when the reinforcing device is in the LII position, an extraordinary reduction is seen, especially in points A and B. Consequently, the optimal device is the one composed of 4 SMA wires positioned at a level of 22.5 m.

5.3 Results after the minaret reinforcement

Here (Figs. 17 and 18), comparisons are drawn for the minaret in its virgin state (without reinforcement) and after that it is reinforced with the 4 SMA wire device positioned at 22.55 m.

According to results found in Table 11, we notice that there is no big change in term of displacement and acceleration between the two studied cases. Regarding the stress reduction, it is clearly noticed that this reduction is significant for points A and B, while it is not important to the point C.

5.4 Reinforcement of the minaret with the SMA device and steel bars

Now, an additional reinforcement case is proposed, just for curiosity. Authors want to know the dynamic behavior of minaret when it will be reinforced with the selected 4 SMA wire device positioned at a level of 40.46 m (LI), in addition to a 4 steel bars device made by the same characteristics of belts used to attach the SMA, previously defined, and positioned at a level of 22.55 m (LII). Results are presented on the Fig. 19 and Fig. 20.

From Table 12, a reduction in terms of stresses and displacements is noticed at point A, but it remains negligible for other positions. By comparing this case to the one of the previous sections (4 SMA wire device located at 22.55 m), this later remains the best.

6. Interpretation of results

6.1 The minaret before being reinforced

The maximum displacement found after applying the El-Centro seismic signal on the minaret is 10 cm. One can conclude that the studied minaret is stiff (as monumental structures), the displacement remains in the security range. A stress concentration is noticed near the balcony area.

6.2 The minaret after being reinforced with the 4 SMA wire device

The dynamic analysis of the minaret when being reinforced with the SMA device near the balcony area shows a slight increase in terms of displacements and accelerations, however, stresses are remarkably reduced in points A and B, thanks to the SMA that allowed the energy dissipation.

Table 11 Result of reinforcement of minaret with 4 SMA

Number of SMA		Without SMA	4 SMA	Difference (%)
Point	Sizes			
A	Ux_{max} (cm)	1.4763	1.49621	-1.34
	Ax_{max} (m/s²)	2.39892	2.38898	0.41
	σx_{max} (MPa)	0.688481	0.213005	69.06
B	Ux_{max} (cm)	4.66844	4.71774	-0.22
	Ax_{max} (m/s²)	4.12924	4.18589	-1.37
	σx_{max} (MPa)	0.438873	0.085637	80.49
C	Ux_{max} (cm)	11.9785	11.9321	0.38
	Ax_{max} (m/s²)	11.6019	11.714	-0.97
	σx_{max} (MPa)	0.018256	0.017617	3.5

Table12 The minaret before and after being reinforced with the two devices

Number of SMA		Without SMA	4 SMA in (A) + 4 Steel in (B)	Difference (%)
Point	Sizes			
A	Ux_{max} (cm)	1.4763	1.157	21.62
	Ax_{max} (m/s²)	2.39892	2.39527	0.15
	σx_{max} (MPa)	0.688481	0.484835	29.5
B	Ux_{max} (cm)	4.66844	4.75808	-1.92
	Ax_{max} (m/s²)	4.12924	4.11565	0.32
	σx_{max} (MPa)	0.438873	0.464605	-5.86
C	Ux_{max} (cm)	11.9785	11.9625	0.13
	Ax_{max} (m/s²)	11.6019	11.4168	1.6
	σx_{max} (MPa)	0.018256	0.018361	-0.6

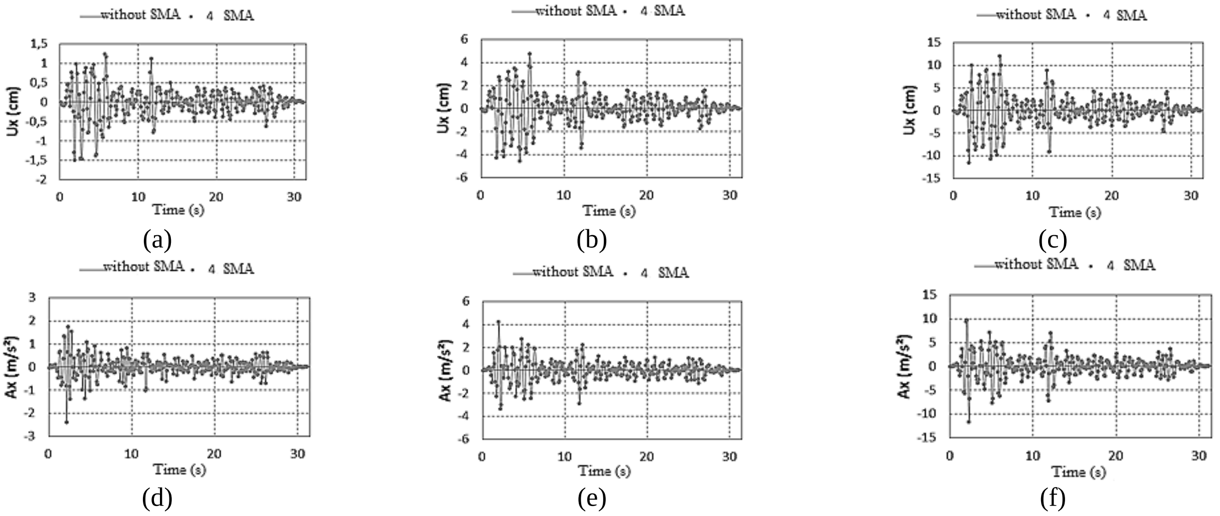

Fig. 17 (a), (b), (c) displacement and (d), (e), (f) acceleration at points A, B, C before and after reinforcement of the minaret

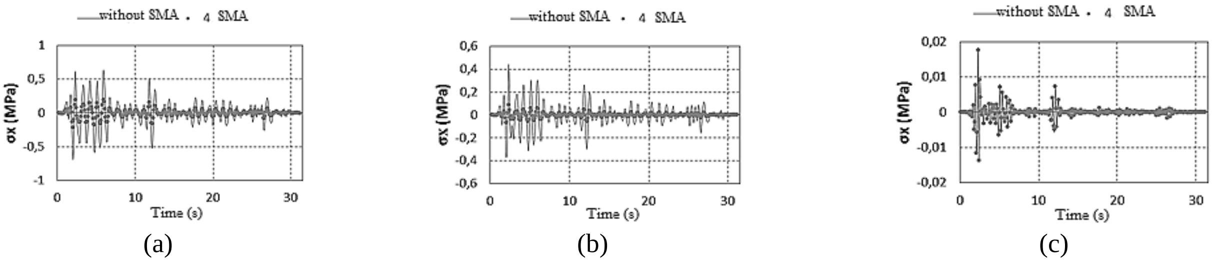

Fig. 18 (a), (b), (c) variation in the stress at points A, B, C before and after reinforcement of the minaret

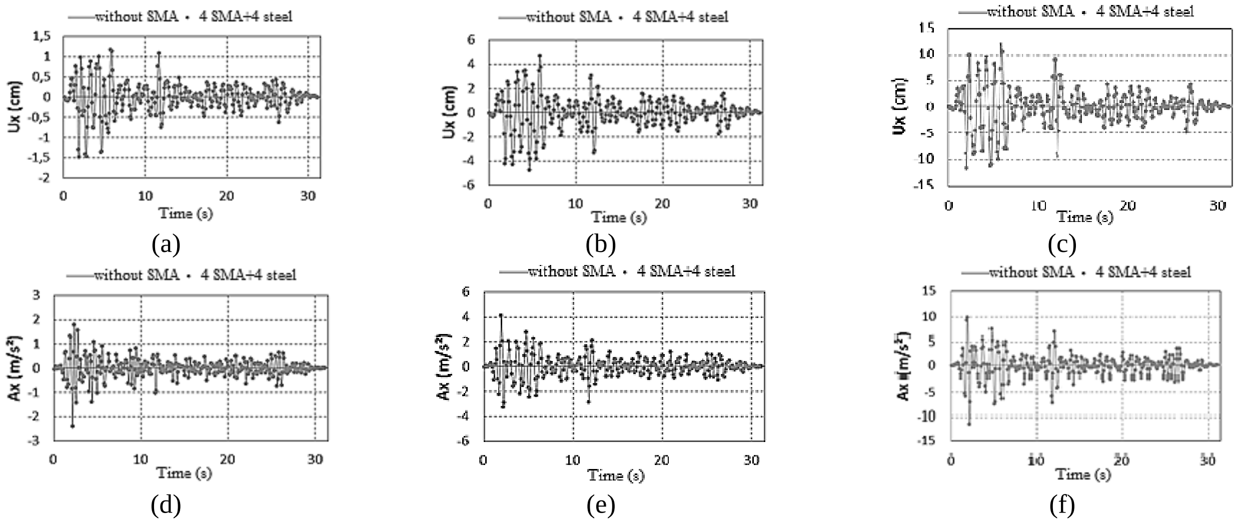

Fig. 19 (a), (b), (c) displacement and (d), (e), (f) acceleration at points A, B, C before and after reinforcing the minaret with two devices

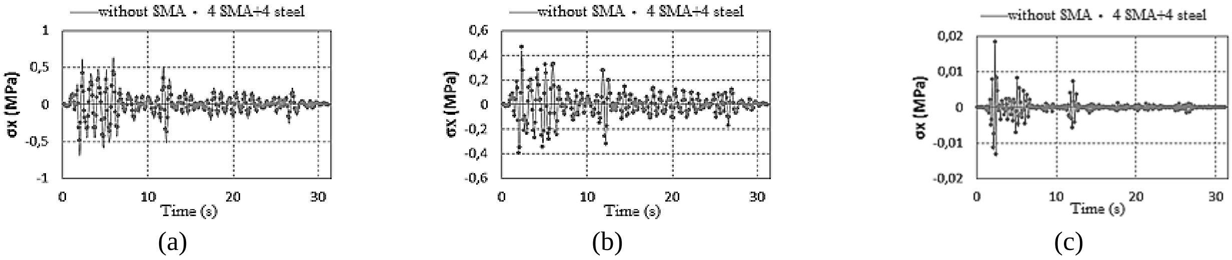

Fig. 20 (a), (b), (c) variation in the stress at points A, B, C before and after reinforcing the minaret with two devices

6.3 The minaret after being reinforced with the two devices

This scenario helps to reduce the stresses near the area of point A. Concerning points B and C, no big changes were seen. Consequently, it is better to use the 4 SMA device positioned at 22.55.

7. Conclusions

The technology based on reinforcing a monumental structure using SMA devices was presented in this contribution. The dynamic behavior of a minaret, before and after the insertion of the SMA devices, was studied by subjecting the monument to the El-Centro seismic signal. Displacements, accelerations and stresses were compared for different scenarios in critical points of the minaret.

Following the drawn analyses, it was demonstrated that the use of the 4 SMA wires device is sufficient instead applying the 8 SMA one. Moreover, the important role of the selected position was confirmed since a reduction of more than 70% was found when the SMA device was fixed at 22.55 m. Furthermore, the additional reinforcing case (SMA device in addition to the steel bars device) may reduce the stresses at the level of point A only. Conversely, for the case of 4 SMA wire device positioned at 22.55 m, a stress reduction was seen for the three points.

It is worth noting that since several combination scenarios concerning the number and the position of devices were tried, analyses time effort was very high. Additionally, and given the complex geometry of the minaret, the proposed way to hang the SMA wires device on the structure was selected to be really applicable and, at the same time, giving the targeted numerical solution.

Finally, one may conclude that the unique ability of SMA to regain their initial shape, the extra energy that they dissipate, their good corrosion resistance and their excellent fatigue behavior justify the pursuit research using these exceptional materials in seismic engineering.

References

AlSaleh, R., Casciati, F., Al-Attar, A. and El-Habbal, I. (2011), “Experimental validation of a shape memory alloy retrofitting application”, *J.Vib. Control*, **18**(1), 28-41.

ANSYS computer software (2003), ANSYS Inc., www.ansys.com.

Azariani, H.R., Esfahani, M.R. and Shariatmadar, H. (2018), “Behavior of exterior concrete beam-column joints reinforced with Shape Memory Alloy (SMA) bars”, *Steel Compos. Struct.*, **28**(1), 83-98.

Bani-Hani, K.A., Zibdeh, H.S. and Hamdaoui, K. (2008), “Health monitoring of a historical monument in Jordan based on ambient vibration test”, *Smart Struct. Syst.*, **4**(2), 195-208.

Ben Jaber, M., Trojette, M.A. and Najar, F. (2015), “A finite element analysis of a new design of a biomimetic shape memory alloy artificial muscle”, *Smart Struct. Syst.*, **16**(3), 479-496.

Casciati, S. and Hamdaoui, K. (2008), “Experimental and numerical studies toward the implementation of shape memory alloy ties in masonry structures”, *Smart Struct. Syst.*, **4**(2), 153-169.

Chrysostomou, C.Z., Stassis, A., Demetriou, T. and Hamdaoui, K. (2008), “Application of shape memory alloy prestressing devices on an ancient aqueduct”, *Smart Struct. Syst.*, .**4**(2), 261-278.

Contreras, M.T., Pasala, D.T.R. and Nagarajaiah, S. (2014), “Adaptive length SMA pendulum smart tuned mass damper performance in the presence of real time primary system stiffness change”, *Smart Struct. Syst.*, **13**(2), 219-233.

Ghawanma, Y.H. (1986), “Ancient Islamic Mosques in Ajloun”, Jordan Center Studies Publications, Al-Yarmouk University, Irbid, Jordan.(In Arabic).

Hamdaoui, K. (2006), “Historical monument health monitoring based on ambient vibrations”; M.Sc. Thesis, Jordan University of Science and Technology, Jordan.

Hamdaoui, K. and Benadla, Z. (2014), “Dynamic analysis of a historical monument: retrofit using shape memory alloy wires”, *Smart Struct. Syst.*, **13**(3), 375-388.

Heresi, P., Herrera, R.A. and Moroni, M.O. (2014), “Testing and modelling of shape memory alloy plates for energy dissipaters”, *Smart Struct. Syst.*, **14**(5), 883-900.

Mehrabi, R. and Karamooz-Ravari, M.R. (2015), “Simulation of superelastic SMA helical springs”, *Smart Struct. Syst.*, **16**(1), 183-194.

Ozbulut, O.E. and Silwal, B. (2016), “Performance assessment of buildings isolated with S-FBI system under near-fault earthquakes”, *Smart Struct. Syst.*, **17**(5), 709-724.

Preciado, A., Ramírez-Gaytan, A., Gutierrez, N., Vargas, D., Falcon, J.M. and Ochoa, J. (2018), “Nonlinear earthquake capacity of slender old masonry structures prestressed with steel, FRP and NiTi SMA tendons”, *Steel Compos. Struct.*, **26**(2), 213-266.

Qiu, C., Zhang, Y., Qi, J. and Li, H. (2018), “Seismic behavior of properly designed CBFs equipped with NiTi SMA braces”, *Smart Struct. Syst.*, **21**(4), 479-491.

Torra, V., Carreras, G., Casciati, S. and Terriault, P. (2014), “On the NiTi wires in dampers for stayed cables”, *Smart Struct. Syst.*, **13**(3), 353-374.

Zhou, X. and You, Z. (2015), “Theoretical analysis of superelastic SMA helical structures subjected to axial and torsional loads”, *Smart Struct. Syst.*, **15**(5), 1271-1291.

FC